Electronic Supplemental Information

Non-conventional low-temperature reverse water–gas shift reaction over highly dispersed Ru catalysts in an electric field

Ryota Yamano[a], Shuhei Ogo[b], Naoya Nakano[a], Takuma Higo[a], and Yasushi Sekine*[a]

Affiliation:

[a] Department of Applied Chemistry, Waseda University, 3-4-1, Okubo, Shinjuku, Tokyo, 169-8555, Japan

[b] Department of Marine Resources Science, Faculty of Agriculture and Marine Science, Kochi University, Nankoku, 783-8502, Japan

Experimental procedure

Table S1. Precursors used for supports synthesis

Atoms / -	Precursor / -
Ti	$[(CH_3)_2CHO]_4Ti$
Zr	$ZrO(NO_3)_2 \cdot 2H_2O$
Ce	$Ce(NO_3)_3 \cdot 6H_2O$
Ca	$Ca(NO_3)_2 \cdot 4H_2O$

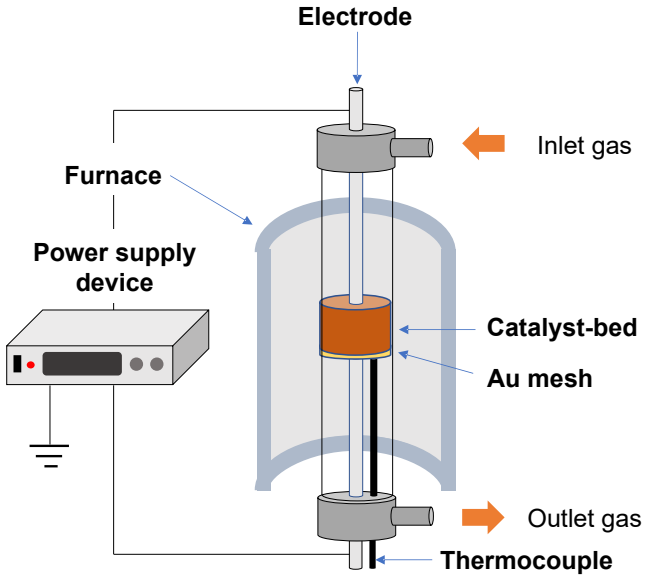

Figure S1. A schematic image of the apparatus for the catalytic activity tests.

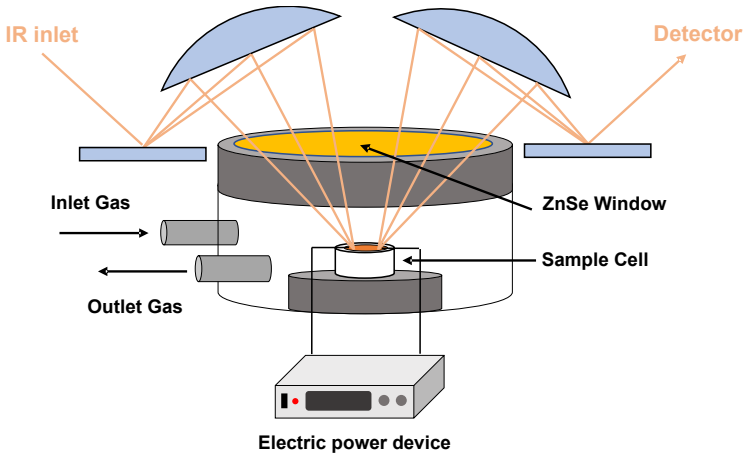

Figure S2. A schematic image of the apparatus for *in-situ* DRIFTS measurements.

Characterisation of the catalysts

To confirm the metal dispersion of catalysts synthesized using different preparation methods, FE-TEM measurements were taken. Representative images of the catalysts and the size distribution of Ru particles are shown in **Figure S3**, demonstrating that the colloidal nanoparticle deposited 1.5wt% $Ru/ZrTiO_4$ catalyst has smaller Ru particles (2.37 nm average particle size) than those of the 1.5wt% $Ru/ZrTiO_4$ catalyst supported by the conventional impregnation method (7.97 nm average particle

size). The image for after the reaction is shown in **Figure S4**, and the catalyst maintained almost the same structure even after the electric field application.

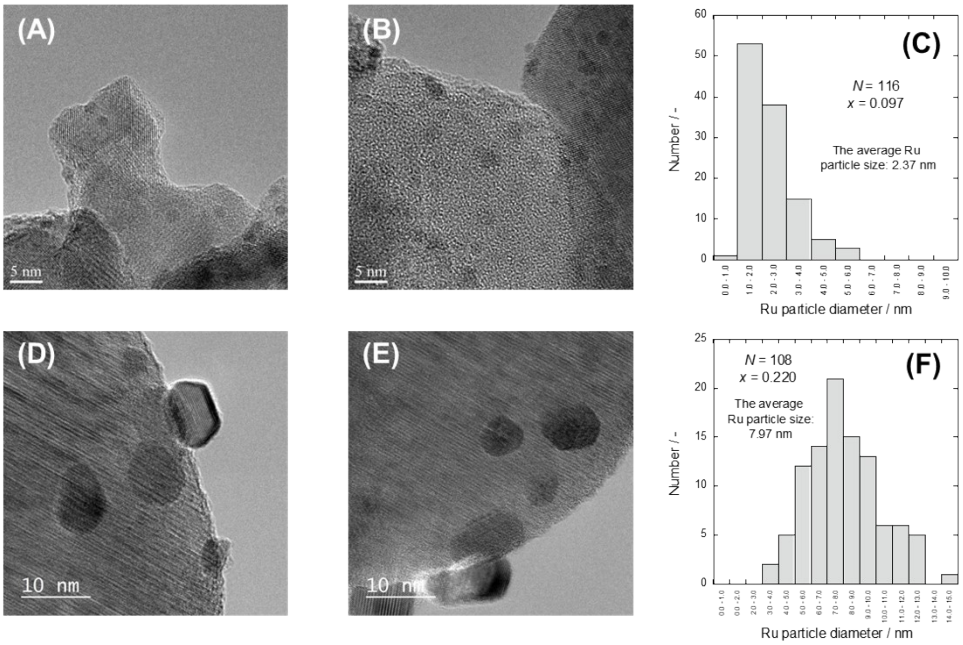

Figure S3. Representative TEM images of (A)-(B) 1.5wt%Ru/$ZrTiO_4$ (colloidal nanoparticles deposited), (D)-(E) 1.5wt% Ru/$ZrTiO_4$ (impregnation method) and (C), (F) corresponding particle size distributions.

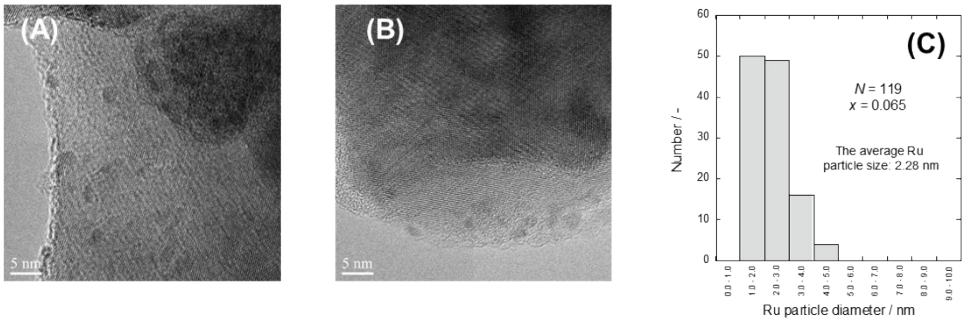

Figure S4. Representative TEM images of (A)-(B) 1.5wt%Ru/$ZrTiO_4$ (colloidal nanoparticles deposited) after the RWGS reaction for 60 minutes with the electric field (CO_2: H_2: Ar = 1: 1: 2; 100 SCCM total flow rate; 5 mA input current) and (C) corresponding particle size distribution.

Activity tests

Table S2. Results of activity tests over various supports (Ru colloidal nanoparticles deposited catalysts) in the electric field

Catalysts*	Temp. / K	Voltage / V	CO_2 conv. / %	CO sel. / %	CO formation rate per input power / mmol kJ^{-1}
1.5wt% $Ru/ZrTiO_4$	511	274	11.2	95.9	1.30
1.7wt% $Ru/Ce_{0.5}Zr_{0.5}O_2$	525	398	11.7	91.9	1.05
1.3wt% $Ru/CaTiO_3$	514	334	12.3	86.2	1.11
2.0wt% Ru/CeO_2 (JRC-CEO-01)	472	160	3.5	94.0	0.638

CO_2: H_2: Ar = 1: 1: 2; 100 SCCM total flow rate; 100 mg catalyst weight; 5.0 mA input current; *the Ru loading weight was evaluated from ICP-OES measurements.

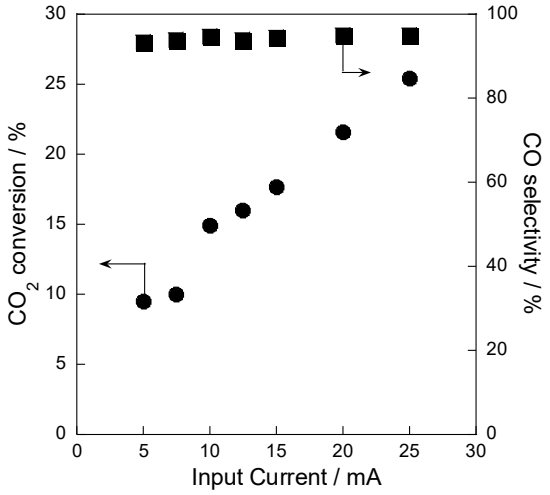

Figure S5. Effects of imposed current on CO_2 conversion and CO selectivity over the Ru(col)/$ZrTiO_4$ catalyst with the electric field at 423 K; CO_2: H_2: Ar = 1: 1: 2; 100 SCCM total flow rate; 100 mg catalyst weight.

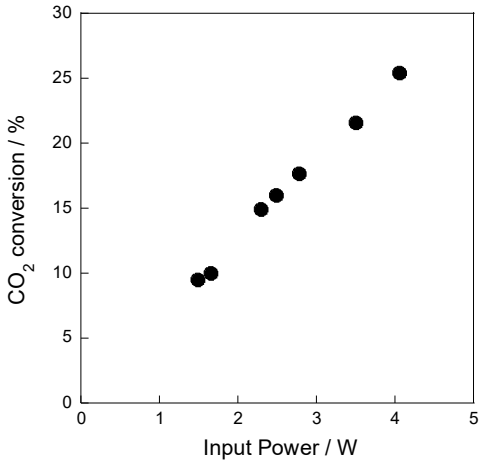

Figure S6. Effects of imposed power on CO_2 conversion over the Ru(col)/$ZrTiO_4$ catalyst with the electric field at 423 K; CO_2: H_2: Ar = 1: 1: 2; 100 SCCM total flow rate; 100 mg catalyst weight.

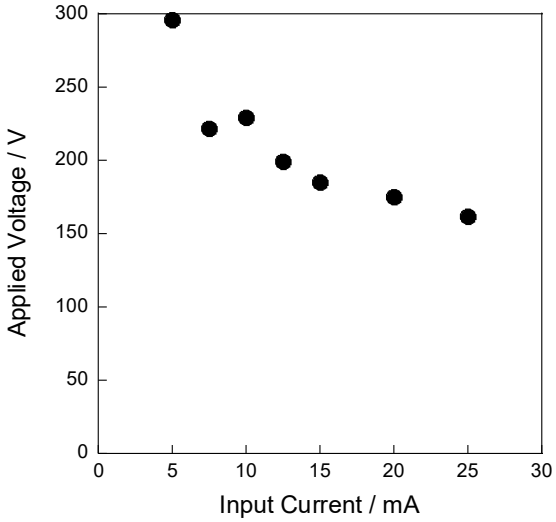

Figure S7. *I-V* characteristic profiles in the electric field over the Ru(col)/$ZrTiO_4$ catalyst at 423 K; CO_2: H_2: Ar = 1: 1: 2; 100 SCCM total flow rate; 100 mg catalyst weight.

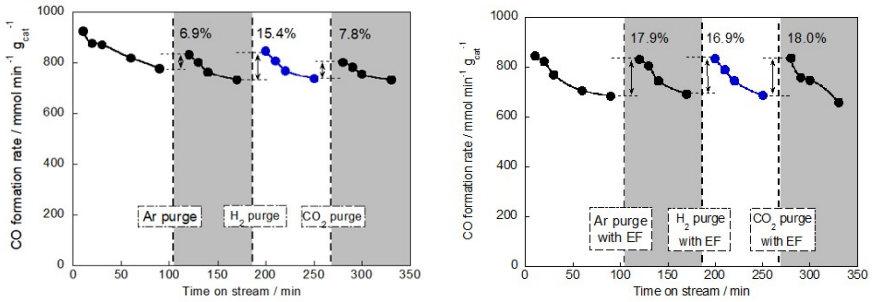

Figure S8. Catalytic stability during the reaction after purge flow (Ar, H_2, CO_2) over the Ru(col)/$ZrTiO_4$ catalyst without the electric field at 593 K (left) and with the electric field (right); CO_2: H_2: Ar = 1: 1: 2; 100 SCCM total flow rate; 100 mg catalyst weight.

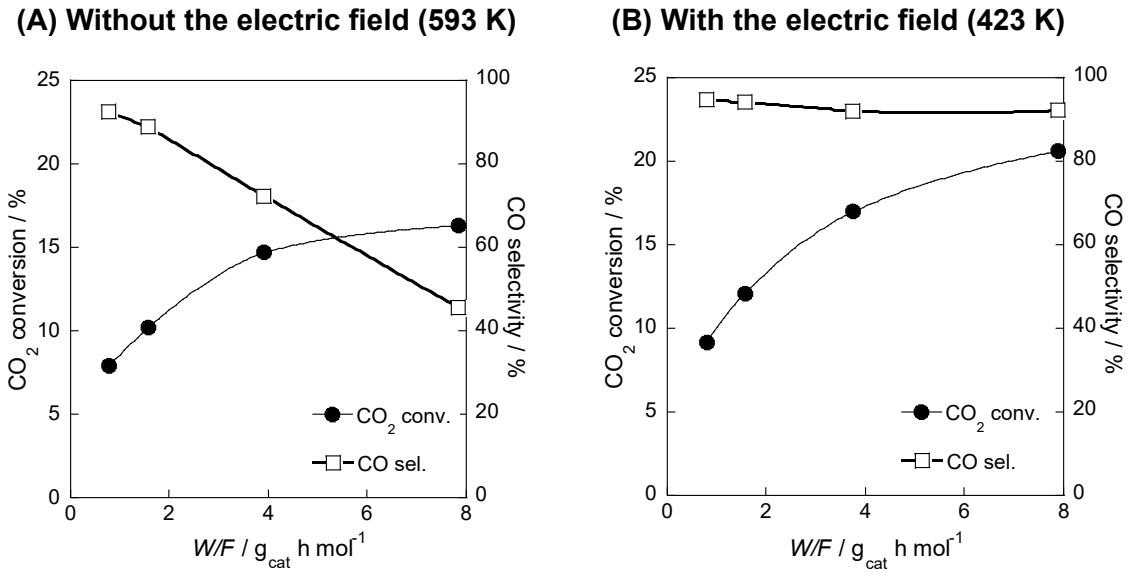

Figure S9. Effect of the contact time (*W*/*F*) on CO_2 conversion and CO selectivity of Ru(col)/$ZrTiO_4$ catalyst (A) without the electric field at 593 K and (B) with the electric field (5 mA) at 423 K; CO_2: H_2: Ar = 1: 1: 2, total flow rate: 20-200 SCCM; input current: 5.0 mA; 100 mg catalyst weight.

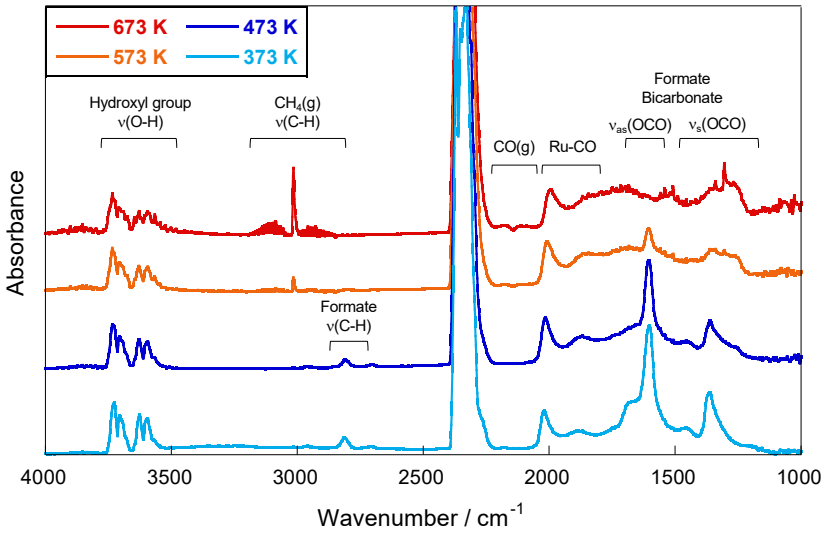

Figure S10. *In-situ* DRIFTS spectra under the RWGS reaction atmosphere over the Ru(col)/$ZrTiO_4$ catalyst without the electric field at 373 K-673 K in all measured wavenumber regions (1000-4000 cm^{-1}).

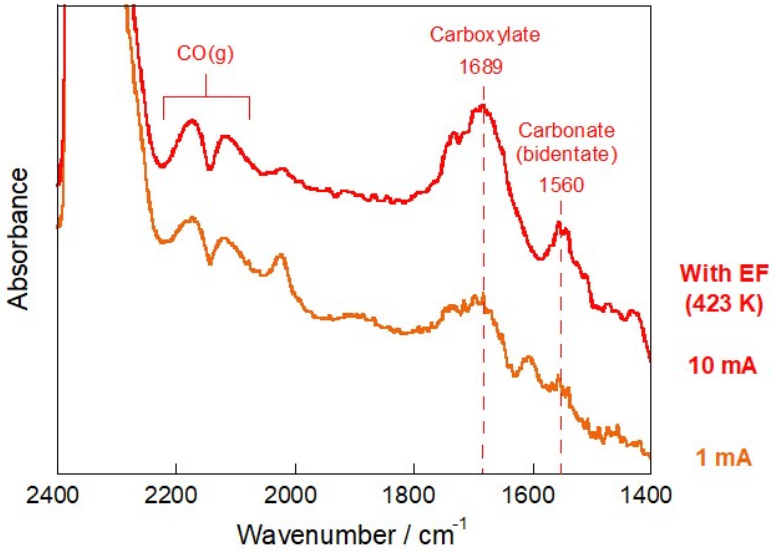

Figure S11. *In-situ* DRIFTS spectra under the RWGS reaction atmosphere over the Ru(col)/$ZrTiO_4$ catalyst recorded during applying the electric field (EF) with different input currents at 423 K; CO_2: H_2: Ar = 1: 1: 2; 40 SCCM total flow rate; 1.0 or 10 mA input current.

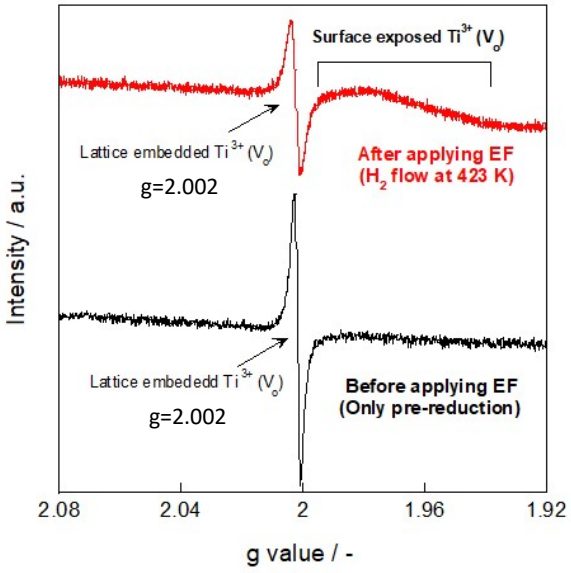

Figure S12. ESR spectra of the Ru(col)/$ZrTiO_4$ catalyst before and after applying the electric field (EF).

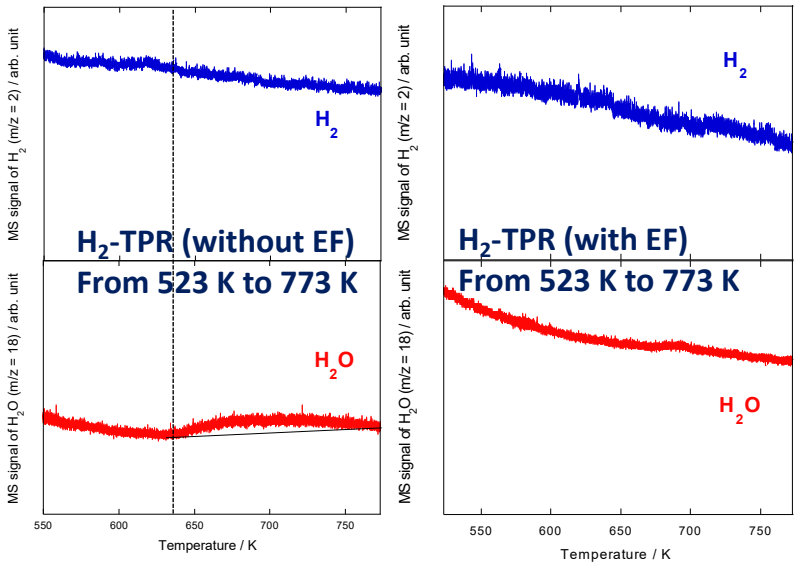

Figure 13. Mass signal of H_2 and H_2O under the reduction atmosphere over the Ru/$ZrTiO_4$ catalyst with/without applying the electric field (EF) at 523-773 K; H_2: Ar = 1: 19, total flow rate: 100 SCCM.

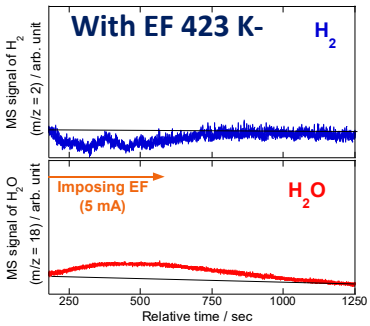

Figure S14. Mass signal of H_2 and H_2O under the reduction atmosphere over the $Ru/ZrTiO_4$ catalyst during applying the electric field (EF) at 423 K; H_2: Ar = 1: 19, total flow rate: 100 SCCM, imposed current: 5.0 mA.